

Supplementary methods:

Chemical reagents:

BYL719(1), GDC0941(2), BKM120(3), AZD1208, GDC0032(4), PI-103(5), BX795(6), BX912(7), MK2206(8), GDC0068(9), sirolimus, everolimus, PP242(10) and WYE354(11) were purchased from Selleck Chemicals.

TCGA analysis of candidate genes' genetic alterations:

Each of the 43 candidate genes was queried through

<http://www.broadinstitute.org/tcga/gistic/browseGisticByGene> for the significance of their copy-number alterations. Significant amplification was defined as q-value less than or equal to 0.25. The q-values of GISTIC 2.0 analysis for the genes with significant amplification were listed in Supplementary Table 2.

Each of the 43 candidate genes was also queried through www.cbioportal.org for their mRNA expression status. For each gene, the number of cases with significant mRNA overexpression or down-regulation (z-score >2 compared to the expression distribution of each gene tumors that are diploid for this gene) was listed in Supplementary Table 2. For each gene, the percent of samples with mRNA upregulation minus percent of samples with mRNA downregulation was calculated. Using an arbitrary cutoff of 6.0%, the genes with the most robust overexpression in this dataset were selected to be tested in MCF7 cells for their ability to confer resistance to GDC0941.

Lentiviral production and infection:

Lentiviral vectors in pLX304 plasmid were obtained from the Broad Institute. Lentiviral particles were produced by cotransfection of HEK 293T cells with pLX304 constructs and packaging plasmids pDelta 8.91 and pVSVG. Transfections were carried out with X-tremeGENE (Roche). Virus was harvested 72 hours after transfection and frozen. Lentivirus was added to cells in the presence of polybrene (4µg/ml). The cell culture plates were spun at 2,250 rpm for 30 minutes at 37°C. The media was then removed 24 hours after infection and fresh media was added. PIM2 ORF was purchased from Harvard PlasmidID (HsCD00040204) as in pDONR221 vector. PIM3 was purchased from GeneCopoeia (GC-Y3334) as in pDONR223 vector. PIM2 and PIM3 were cloned using Gateway cloning protocol to

pLX304 expression vector.

Statistical analysis of ORF screen:

For each ORF, the infection efficiency was calculated as the ratio of raw luminescence from CellTiterGlow (CTG) for cells selected with blasticidin to the raw luminescence for unselected cells. ORFs with an infection efficiency of greater than 0.65 were considered sufficient infections and were analyzed subsequently. 15,179 of 15,970 (95.05%) ORFs met our infection efficacy criteria. CTG luminescence values for cells expressing each ORF in the presence of BYL719 were compared to the mean and standard deviation for all ORF-expressing cells on the same 384-well plate by calculating a standard score (or z-score) for each ORF. Average z-score was calculated using the treatment duplicate. A z-score ≥ 2.5 was used to select ORFs that are associated with proliferation in the presence of the drug for validation.

Colony-formation assays:

Cells were plated to 12-well plate at 1,000 – 3,000 cells per well density and infected with lentivirus the next day. After another 24 hours, media was changed to remove lentivirus. Drug or DMSO was added to each well. Drug containing media was refreshed every 3 days. After 18-21 days of drug treatment, cells were then fixed with cold methanol and stained with 0.5% crystal violet solution. Cells were de-stained using 10% SDS and crystal violet uptake was measured at 595 nm for quantification.

Cell cycle analysis:

Cells were harvested and washed with PBS. They were then fixed in cold 70% ethanol for two hours at -20°C . Two additional washes were performed using PBS with spin at 1000 rpm for 5 minutes. Propidium iodide staining buffer 200 μl (PI: 20 $\mu\text{g}/\text{ml}$ and RNase A:0.2mg/ml in PBS/triton) was then added to each sample with another 300 μl of PBS. Flow cytometry was performed using BD LSRFortessa at the wavelength of 605nm. The FCS files were analyzed using the ModFit software to generate the percentage of cells in each cell cycle phase. The histogram graphs were generated using the FlowJo single cell analysis software.

RNA-sequencing in T47D cells:

Total RNA from T47D cells without infection and with PIM1 or GFP overexpression was extracted using RNeasy Kit (QIAGEN). 200 ng of total RNA from each sample was used for starting material. Oligo dT beads were used to select mRNA from the total RNA. The selected RNA was then heat fragmented and randomly primed before cDNA synthesis from the RNA template. The resultant cDNA then went through Illumina library prep (end repair, base 'A' addition, adapter ligation, and enrichment) using Broad designed indexed adapters for multiplexing. After enrichment, the samples were qPCR quantified and equimolar pooled before proceeding to Illumina sequencing (Illumina HiSeq) with sequence coverage to 50M paired reads and 100M total reads. This standard non-strand specific RNA sequencing protocol at the Broad Institute uses a large-scale, automated variant of the Illumina TruSeq™ RNA Sample Preparation protocol.

RNA-sequencing data analysis:

Reads were mapped to the reference human genome (hg19) using TopHat 1.4.1. Expression levels for each gene were denoted as RPKM (reads per kilobase of transcript per million mapped reads) values determined using Cufflinks 2.0.2. The RPKM values were then log₂ transformed. Genes with low expression in all the samples (log₂ RPKM < -1) were excluded in downstream analysis. Heatmap in Fig 5A of each gene was generated using RPKM values in all the successfully sequenced tumor samples in GeneE.

Single-sample Gene Set Enrichment Analysis:

Single-sample GSEA (ssGSEA) is an extension of Gene Set Enrichment Analysis (GSEA) that was developed in the Broad Institute (Barbie et al 2009). It calculates an enrichment score for each sample against one gene set. The ssGSEA enrichment score represents the degree to which the genes in this gene set are coordinately up- or down-regulated within a sample. The analysis tool is available at <http://www.broadinstitute.org/cancer/software/genepattern/> In order to generate a PIM signature, RNA-seq based expression profiles of T47D cells with PIM1 overexpression was compared to control (GFP-expressing) cells and uninfected parental cells. The PIM signature was defined as the top 37 differentially upregulated genes together with PIM1, 2, 3, and the top 47 differentially downregulated

genes (FDR<10%) were defined as a PIM activation signature (Supplementary Fig. S6). For pt 4 and 5, for each of the signature gene, the change of the gene was calculated using RPKM values from post-treatment samples divided by RPKM values from pre-treatment samples. A change greater than 1.5 fold was designated as upregulated, whereas a change less than 0.667 fold was designated as downregulated. A change between 0.667 – 1.5 was designated as no change. For each patient, a subset of genes was found to change concordantly with the PIM signature. Those genes are likely the primary contributory genes driving the positive correlation of PIM1 signature in those two patients.

Supplementary references:

1. Furet P, Guagnano V, Fairhurst RA, Imbach-Weese P, Bruce I, Knapp M, et al. Discovery of NVP-BYL719 a potent and selective phosphatidylinositol-3 kinase alpha inhibitor selected for clinical evaluation. *Bioorg Med Chem Lett*. 2013 Jul 1;23(13):3741–8.
2. Folkes AJ, Ahmadi K, Alderton WK, Alix S, Baker SJ, Box G, et al. The identification of 2-(1H-indazol-4-yl)-6-(4-methanesulfonyl-piperazin-1-ylmethyl)-4-morpholin-4-yl-thieno[3,2-d]pyrimidine (GDC-0941) as a potent, selective, orally bioavailable inhibitor of class I PI3 kinase for the treatment of cancer. *J Med Chem*. 2008 Sep 25;51(18):5522–32.
3. Burger MT, Pecchi S, Wagman A, Ni Z-J, Knapp M, Hendrickson T, et al. Identification of NVP-BKM120 as a Potent, Selective, Orally Bioavailable Class I PI3 Kinase Inhibitor for Treating Cancer. *ACS Med Chem Lett*. 2011 Oct 13;2(10):774–9.
4. Ndubaku CO, Heffron TP, Staben ST, Baumgardner M, Blaquiére N, Bradley E, et al. Discovery of 2-{3-[2-(1-isopropyl-3-methyl-1H-1,2,4-triazol-5-yl)-5,6-dihydrobenzo[f]imidazo[1,2-d][1,4]oxazepin-9-yl]-1H-pyrazol-1-yl}-2-methylpropanamide (GDC-0032): a β -sparing phosphoinositide 3-kinase inhibitor with high unbound exposure and robust in vivo antitumor activity. *J Med Chem*. 2013 Jun 13;56(11):4597–610.
5. Fan Q-W, Knight ZA, Goldenberg DD, Yu W, Mostov KE, Stokoe D, et al. A dual PI3 kinase/mTOR inhibitor reveals emergent efficacy in glioma. *Cancer Cell*. 2006 May;9(5):341–9.
6. Clark K, Plater L, Peggie M, Cohen P. Use of the pharmacological inhibitor BX795 to study the regulation and physiological roles of TBK1 and I κ B kinase epsilon: a distinct upstream kinase mediates Ser-172 phosphorylation and activation. *J Biol Chem*. 2009 May 22;284(21):14136–46.
7. Feldman RI, Wu JM, Polokoff MA, Kochanny MJ, Dinter H, Zhu D, et al. Novel small molecule inhibitors of 3-phosphoinositide-dependent kinase-1. *J Biol Chem*. 2005 May 20;280(20):19867–74.
8. Hirai H, Sootome H, Nakatsuru Y, Miyama K, Taguchi S, Tsujioka K, et al. MK-2206, an allosteric Akt inhibitor, enhances antitumor efficacy by standard chemotherapeutic agents or molecular targeted drugs in vitro and in vivo. *Mol Cancer Ther*. 2010 Jul;9(7):1956–67.
9. Lin J, Sampath D, Nannini MA, Lee BB, Degtyarev M, Oeh J, et al. Targeting activated Akt with GDC-0068, a novel selective Akt inhibitor that is efficacious in multiple tumor models. *Clin Cancer Res Off J Am Assoc Cancer Res*. 2013 Apr 1;19(7):1760–72.
10. Feldman ME, Apsel B, Uotila A, Loewith R, Knight ZA, Ruggiero D, et al. Active-site inhibitors of mTOR target rapamycin-resistant outputs of mTORC1 and mTORC2. *PLoS Biol*. 2009 Feb 10;7(2):e38.
11. Yu K, Toral-Barza L, Shi C, Zhang W-G, Lucas J, Shor B, et al. Biochemical, cellular, and in vivo activity of novel ATP-competitive and selective inhibitors of the mammalian target of rapamycin. *Cancer Res*. 2009 Aug 1;69(15):6232–40.

Supplementary figures and tables:

S. Table 1. Functional classification for validated genes

Functional groups	Gene names
Growth factors	<i>NRG1, FGF3, FGF10,</i>
GPCR	<i>GPR161</i>
GTPase/GEF	<i>TBC1D3G, RIC8A</i>
Tyrosine kinases	<i>DYRK1B, AXL, ITGB1BP3, SRC, CDK5R1</i>
Serine-Threonine kinases	<i>PRKACA, PIM1 PIM3, PRKCZ, AKT1, PDK1, AKT2, CCND1</i>
Phosphatases	<i>PPP1R3B</i>
Adapter proteins	<i>CRKL, CRB3, SRP54</i>
Transcription factors/co-factors	<i>YAP1, ZSCAN20, SMAD5, SAMD4B</i>
Metabolic process	<i>B4GALT6, NUDT3, NUDT10(?)</i>
Other	<i>CXorf41(PIH1D3), MFSD5, C9orf24 (SMRP1), C1QL2, PLEKHF1, GOLGA1, KCNIP1, PSMD13, PRAMEF9, USP38, SLC6A20, OSTalpha</i>

S. Table 2. Validated 43 candidate genes' genetic alteration status in the invasive breast cancer (TCGA) database. 7 genes have significant amplification by GISTIC 2.0 analysis ($q > 0.25$). 17 genes have mRNA up – mRNA down in more than 6.0% of the cases. Some genes have both amplification and overexpression; total of 18 genes were found to be amplified and/or overexpressed in this dataset.

Gene names	Amp	GISTIC 2.0 q-value	Del	Mut	mRNA up	mRNA down	Total alterations	% Total alterations
NRG1	29	-	42	2	22	0	95	9.9
FGF3	143	2.55E-164	0	2	10	0	154	16.0
FGF10	18	-	3	2	30	0	53	5.5
GPR161	102	1.90E-05	2	5	112	0	177	18.4
TBC1D3G	31	0.0148	4	0	0	0	35	3.6
RIC8A	1	-	13	6	44	60	114	11.9
DYRK1B	26	-	2	1	44	3	63	6.6
AXL	15	-	3	7	45	0	67	7.0
ITGB1BP3 (NMRK2)	7	-	4	1	1	0	13	1.4
SRC	23	-	0	1	110	2	120	12.5
CDK5R1	29	7.71E-04	4	1	63	0	87	9.1
PRKACA	16	-	0	2	56	12	78	8.1
PIM1	15	-	0	0	77	0	74	7.7
PIM3	7	-	10	2	32	0	47	4.9
PRKCZ	8	-	10	2	46	11	72	7.5
AKT1	17	-	3	2	84	8	103	10.7
PDK1	6	-	1	2	64	0	72	7.5
AKT2	23	-	2	4	84	16	111	11.6
CCND1	152	2.25E-178	0	1	147	0	213	22.2
PPP1R3B	5	-	60	2	35	1	102	10.6
CRKL	13	-	1	1	49	43	101	10.5
CRB3	6	-	5	1	58	5	74	7.7
SRP54	19	0.0544	0	1	104	32	138	14.4
YAP1	5	-	13	1	31	32	79	8.2
ZSCAN20	8	-	2	3	35	1	45	4.7
SMAD5	3	-	3	2	41	27	71	7.4
SEMA4B	31	-	1	1	61	0	83	8.6
B4GALT6	10	-	1	2	71	0	77	8.0
NUDT3	13	-	0	1	102	0	110	11.5
NUDT10	10	-	3	2	23	0	38	4.0
CXorf41(PIH1D3)	3	-	2	1	14	0	20	2.1
MFSD5	2	-	0	0	68	2	71	7.4
C9orf24	13	-	0	1	26	0	39	4.1
C1QL2	2	-	0	0	26	0	27	2.8
GOLGA1	15	-	1	5	46	68	126	13.1

KCNIP1	9	-	5	1	16	0	31	3.2
PSMD13	1	-	15	0	55	0	70	7.3
PRAMEF9	4	-	7	0	4	0	15	1.6
USP38	8	-	0	2	56	6	64	6.7
SLC6A20	1	-	5	0	43	0	48	5.0
CMTM2	3	-	13	0	54	0	70	7.3
OSTalpha	0	0.0012	0	0	46	0	46	4.8
PLEKHF1	41	-	3	1	75	0	96	10

S. Table 3. Receptor status, mutational status and intrinsic subtypes of breast cancer cell lines used in this study.

Cell line	Intrinsic subtype	Molecular characteristics				
		<i>PIK3CA</i>	<i>PTEN</i>	ER	PR	HER2
T47D	luminal A	H1047R	-	+	+	-
MCF7	luminal A	E545K	-	+	+	-
EFM19	luminal A	H1047L	-	+	?	-
BT474	luminal-B	K111N	-	+	+	amp
MDAMB453	HER2-enriched	H1047R	E307K	-	-	amp
HCC202	HER2-enriched	E545K and L866F	-	-	-	amp
MDAMB361	luminal-B	E545K and K567R	-	+	+	amp
HCC1419	luminal-B	-	-	+	-	amp
MDAMB415	luminal-A	-	C136Y	+	+	-
HCC1937	basal-like	-	homo del	-	-	-
UACC893	HER2-enriched	H1047R	-	-	-	amp
BT483	luminal-A	E542K	-	+	-	-
JIMT1	HER2-enriched	C420R	-	-	-	amp
HCC1954	HER2-enriched	H1047R	-	-	-	amp
BT20	basal-like	P539R and H1047R	-	-	-	-
CAL51	basal-like	E542K	E288fs*, T321fs	-	-	-

* Deletion - Frameshift

S. Table 4. GI₅₀ of BYL719 in different breast cancer cell lines with overexpression of PIM isoforms

Cell line	Genes	BYL719 GI ₅₀ (uM)	fold change PIM/GFP
T47D	GFP	0.25	-
	PIM1	0.92	3.68
MCF7	GFP	0.17	-
	PIM1	1.69	10.05
BT474	GFP	0.64	-
	PIM1	1.68	2.63
MDAMB453	GFP	0.6	-
	PIM1	1.7	2.82
EFM	GFP	0.037	-
	PIM1	0.28	7.57
HCC202	GFP	0.12	-
	PIM1	0.94	7.83
HCC1419	GFP	7.71	-
	PIM1	>10	NA
HCC1937	GFP	>10	-
	PIM1	>10	NA
MDAMB415	GFP	>10	-
	PIM1	>10	NA
Cell line	Genes	BYL719 GI ₅₀ (uM)	fold change PIM/GFP
T47D	GFP	0.15	-
	PIM1	0.70	4.67
	PIM2	0.36	2.43
	PIM3	0.19	1.29

S. Table 5. PIM1 and AKT phosphorylation sites in PRAS40, BAD, p21 and p27

PIM1 substrate preference	L/KRRXS*/T*
AKT substrate preference	RXRXXS*/T*
Common targets of PIM1 and AKT	Consensus site
PRAS40 T246	RPRLNT*
BAD S112	LRRMS*
p21 T145	RKRRQT*S
p27 T157	RKRPAT*

S. Table 6. PIM gene expression levels in *PIK3CA*-mutant breast cancer cell lines

Resistant cell lines	PIM1 expression (log2)	PIM2 expression (log2)	PIM3 expression (log2)
JIMT1	7.83	7.13	9.07
HCC1954	7.55	6.12	8.63
BT20	7.55	5.21	9.43
CAL51	7.11	5.84	8.56
Sensitive cell lines	PIM1 expression (log2)	PIM2 expression (log2)	PIM3 expression (log2)
MCF7	6.72	6.42	9.47
UACC893	6.27	5.73	10.08
T47D	6.00	6.55	8.52
HCC202	6.00	5.75	8.46
EFM19	5.99	5.79	8.86
MDAMB361	5.81	6.24	9.90
BT483	5.45	5.83	10.71
BT474	5.27	6.02	9.54
MDAMB453	4.88	6.07	9.38

S. Table 7. GI₅₀ of BYL719 in the presence of LGH447 (1μM) or DMSO in *PIK3CA*-mutant breast cancer cell lines.

	LGH447 (BYL719 GI₅₀ μM)	DMSO (BYL719 GI₅₀ μM)	Fold change DMSO/LGH447
CAL51	2.07	5.72	2.77
JIMT1	2.93	12.77	4.36
HCC1954	1.22	2.56	2.09
BT20	3.48	3.98	1.14
T47D	0.19	0.24	1.28
EFM19	0.29	0.38	1.32

S. Table 8. Signature genes that changed concordantly in patient sample pairs and PIM signature.

pt 4	pt 5
Up-regulated genes	
PIM1	PIM3
PIM2	THRSP
PIM3	STEAP1
STEAP1	HGD
SPRY4	CLGN
LAT2	GDF15
SLC7A11	AZGP1P1
SFMBT2	SLC7A11
DUSP5	AZGP1
RAB39B	RAB39B
IL6R	IL6R
HK2	HK2
FAM46C	ST3GAL1
WARS	ENPP1
SESN2	TRIB3
	SLC31A1
	KIAA1244
Down-regulated genes	
HAUS5	HAUS5
CYP2U1	LPCAT1
KATNAL2	CYP2U1
MAP6D1	KATNAL2
PYROXD2	ENDOV
ENDOV	TELO2
LTBP2	ADM
TMEM143	LTBP2
FZD2	TMEM143
WTIP	LHFP
C11orf31	FZD2
ME3	WTIP
C1QTNF6	CHTF18
NME3	ME3
	MXD3

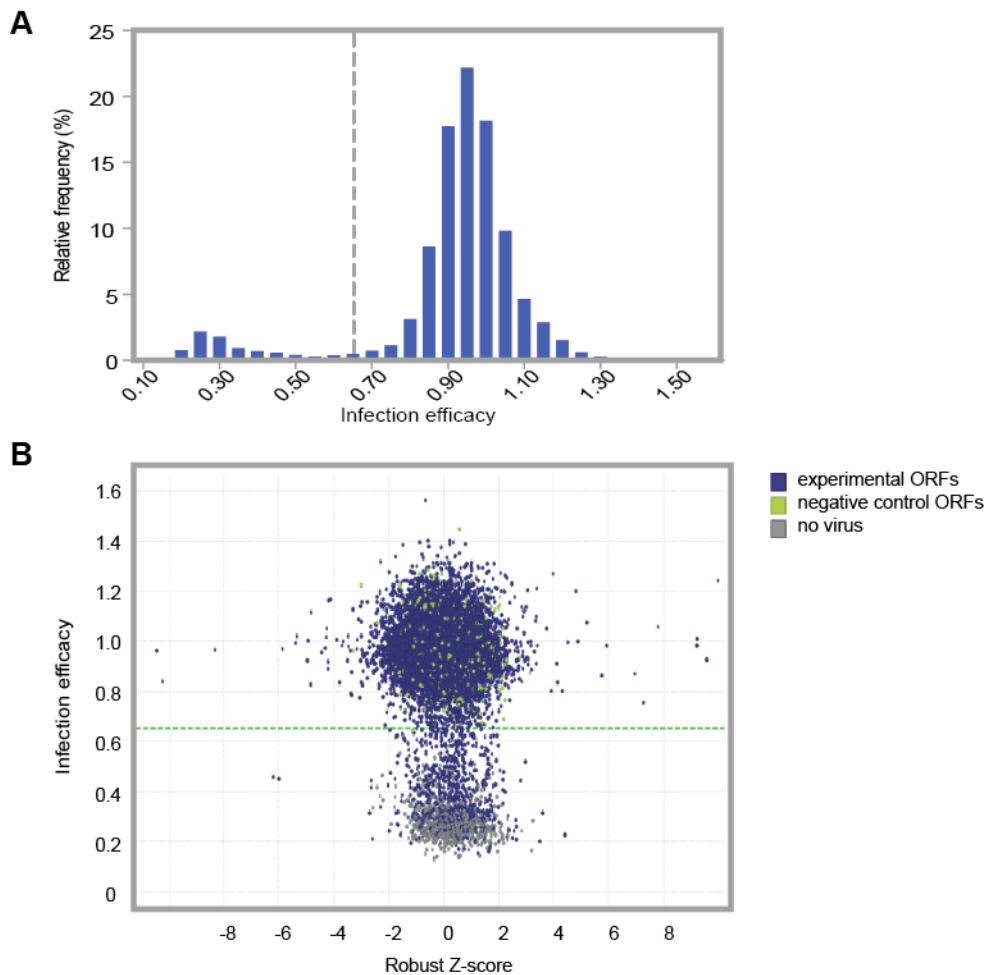
S Table 9. Hormonal receptor status by immunohistochemistry (IHC), HER2 status by FISH and IHC of PIM1 amplified or overexpressed breast cancer tumor samples from the invasive breast cancer (TCGA) database. Total of 74 cases have PIM1 amplification and/or overexpression. Among them, 28 samples had luminal or HER2-enriched subtypes based on receptor status from clinical reports, 45 samples were basal-like, 1 case was not evaluable.

Patient.ID	ER.by IHC	PR.by .IHC	HER2.fish. status	IHC.HER2	PIM1 status	PIK3CA status	Subtype
TCGA-AR-A0TS	-	-	NE	-	Amp	-	basal
TCGA-A7-A4SE	-	-	NE	-	Amp	Amp	basal
TCGA-BH-A0AV	-	-	-	NA	Amp	-	basal
TCGA-C8-A27B	-	-	NE	-	Amp	-	basal
TCGA-E9-A1NC	-	+	NE	+	Amp	-	luminal
TCGA-BH-A0W7	+	+	NE	-	Amp	H1047R, E726K	luminal
TCGA-A2-A04U	-	-	+	-	Amp	-	HER2
TCGA-A2-A4S1	+	-	NE	-	Amp	-	luminal
TCGA-A8-A08F	+	+	-	-	Amp	-	luminal
TCGA-AN-A0AT	-	-	NE	-	Amp	-	basal
TCGA-BH-A5IZ	+	-	-	-	Amp	-	luminal
TCGA-C8-A1HJ	-	-	NE	-	Amp	-	basal
TCGA-D8-A142	-	-	-	Equivocal	Amp	-	basal
TCGA-D8-A27W	+	+	+	Equivocal	Amp	-	luminal
TCGA-E9-A22G	-	-	NE	+	Amp	-	HER2
TCGA-A2-A04T	-	-	-	Equivocal	Over-expr	Amp,H1047Y	basal
TCGA-A2-A3XY	-	-	-	-	Over-expr	Amp, Over-expr	basal
TCGA-BH-A18V	-	-	NA	-	Over-expr	Amp, Over-expr	basal
TCGA-D8-A27H	-	-	NE	-	Over-expr	Amp, Over-expr	basal
TCGA-OL-A5RW	-	-	-	NE	Over-expr	Amp	basal
TCGA-BH-A0BO	+	+	NA	-	Over-expr	H1047R	luminal
TCGA-OL-A5S0	+	-	+	NE	Over-expr	E542K	luminal
TCGA-A2-A0SX	-	-	NE	-	Over-expr	Over-expr	basal
TCGA-A2-A0YM	-	-	-	NE	Over-expr	Over-expr	basal
TCGA-A2-A25F	-	+	NE	-	Over-expr	Over-expr	luminal
TCGA-AC-A2BK	-	-	NE	-	Over-expr	Over-expr	basal
TCGA-BH-A0BL	-	-	NA	-	Over-expr	Over-expr	basal
TCGA-D8-A1XW	-	+	NE	-	Over-expr	Over-expr	luminal
TCGA-E2-A150	-	-	NE	-	Over-expr	Over-expr	basal
TCGA-A1-A0SK	-	-	NE	-	Over-expr	-	basal
TCGA-A2-A0CM	-	-	NE	-	Over-expr	-	basal
TCGA-A2-A0CO	+	+	-	-	Over-expr	-	luminal
TCGA-A2-A0EP	+	-	-	-	Over-expr	-	luminal
TCGA-A2-A0YJ	+	-	NE	-	Over-expr	-	luminal
TCGA-A2-A3XS	-	-	-	NE	Over-expr	-	basal
TCGA-A2-A3XX	-	-	-	-	Over-expr	-	basal

TCGA-A2-A3Y0	+	-	NE	-	Over-expr	-	luminal
TCGA-A2-A4RX	+	+	NE	-	Over-expr	-	luminal
TCGA-A7-A13E	+	-	-	Equivocal	Over-expr	-	luminal
TCGA-A7-A5ZV	-	-	-	Equivocal	Over-expr	-	basal
TCGA-AC-A23G	+	+	+	+	Over-expr	-	luminal
TCGA-AN-A0FN	+	+	NE	+	Over-expr	-	luminal
TCGA-AN-A0FX	-	-	NE	+	Over-expr	-	HER2
TCGA-AO-A0JC	+	+	NE	-	Over-expr	-	luminal
TCGA-AR-A1AQ	-	-	-	Equivocal	Over-expr	-	basal
TCGA-AR-A24W	+	+	NE	-	Over-expr	-	luminal
TCGA-AR-A2LR	-	-	NE	-	Over-expr	-	basal
TCGA-B6-A0I1	-	-	NE	NE	Over-expr	-	basal
TCGA-B6-A0IA	+	+	NA	NE	Over-expr	-	luminal
TCGA-B6-A0IJ	+	+	NA	NE	Over-expr	-	luminal
TCGA-B6-A0RT	-	-	NA	NE	Over-expr	-	basal
TCGA-B6-A0WX	-	-	NE	NE	Over-expr	-	basal
TCGA-B6-A400	-	-	NE	-	Over-expr	-	basal
TCGA-B6-A402	-	-	NE	-	Over-expr	-	basal
TCGA-B6-A409	-	-	-	Equivocal	Over-expr	-	basal
TCGA-BH-A1FC	-	-	NA	-	Over-expr	-	basal
TCGA-D8-A27F	-	-	NE	-	Over-expr	-	basal
TCGA-E2-A108	+	+	NE	-	Over-expr	-	luminal
TCGA-E2-A14R	-	-	NE	-	Over-expr	-	basal
TCGA-E2-A14X	-	-	NE	-	Over-expr	-	basal
TCGA-E2-A1LG	-	-	-	Equivocal	Over-expr	-	basal
TCGA-E2-A1LH	-	-	NE	-	Over-expr	-	basal
TCGA-E2-A1LI	-	-	-	Equivocal	Over-expr	-	basal
TCGA-E9-A3QA	NE	NE	NE	NE	Over-expr	-	NE
TCGA-E9-A5FL	-	-	NE	-	Over-expr	-	basal
TCGA-EW-A1P1	-	-	-	Equivocal	Over-expr	-	basal
TCGA-EW-A1P7	-	-	-	Equivocal	Over-expr	-	basal
TCGA-EW-A1PH	-	-	NE	-	Over-expr	-	basal
TCGA-GM-A2DF	-	-	-	-	Over-expr	-	basal
TCGA-HN-A2NL	-	-	NE	-	Over-expr	-	basal
TCGA-LL-A440	+	+	-	Equivocal	Over-expr	-	luminal
TCGA-LL-A441	-	-	NE	-	Over-expr	-	basal
TCGA-LL-A5YP	+	-	+	-	Over-expr	-	luminal
TCGA-OL-A66I	-	-	-	NE	Over-expr	-	basal

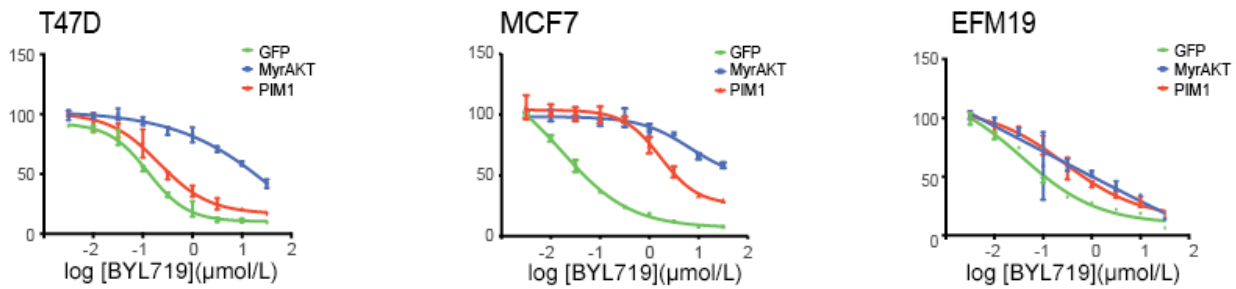
NE: not evaluable, Amp: amplified, Over-expr: mRNA overexpression

S. Figure 1. Lentiviral infection efficacy quality in the large-scale ORF screen. **A.** Infection efficacy (IE) distribution for all the ORFs arrayed in the screen. IE was calculated as the ratio of raw CTG of cells treated with blasticidin (selectable marker harbored by the lentiviral expression vector) to CTG of cells in DMSO. Data is shown for all experimental ORFs, negative control ORFs, and no viral controls. **B.** Infection efficiency (IE) and Z-score for all the ORFs arrayed in the screen. No viral uninfected cells lack the blasticidin selectable marker and are therefore associated with low calculated IE (grey dots). Experimental ORFs with IE <0.65 were considered failed infections and were not further analyzed.

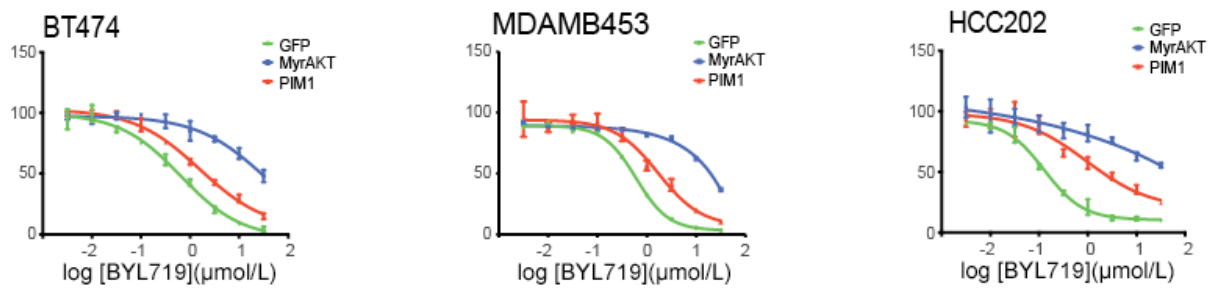


S. Figure 2. PIM1 confers resistance to breast cancer cell lines with different *PIK3CA* mutations and various intrinsic subtypes. Different breast cancer cells with (A) luminal A with *PIK3CA* mutations (B) luminal B subtype with *PIK3CA* mutation, (C) HER2-enriched subtype with *PIK3CA* mutations, and (D) HER2-enriched without *PIK3CA* mutation, (E) *PTEN* loss-of-function, were infected with lentivirus of GFP, PIM1, or myrAKT. The cells were treated with various doses of BYL719 for 3 days. Cell proliferation was determined by MTS assay. Mean and SE of three replicates are shown.

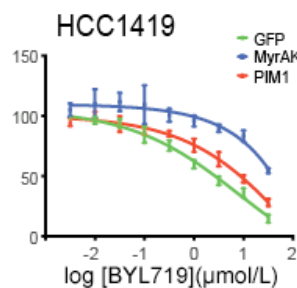
A Luminal A with *PIK3CA* mutations



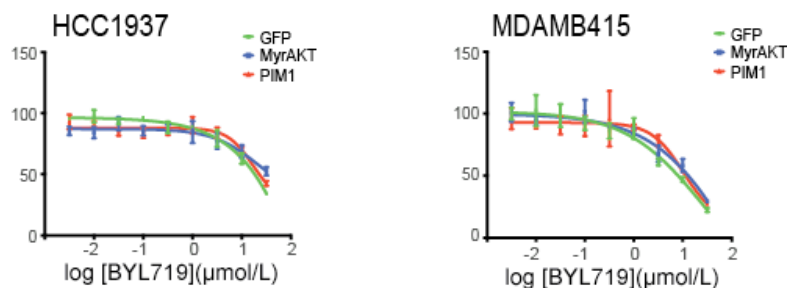
B Luminal-B with *PIK3CA* mutations C HER2-enriched with *PIK3CA* mutations



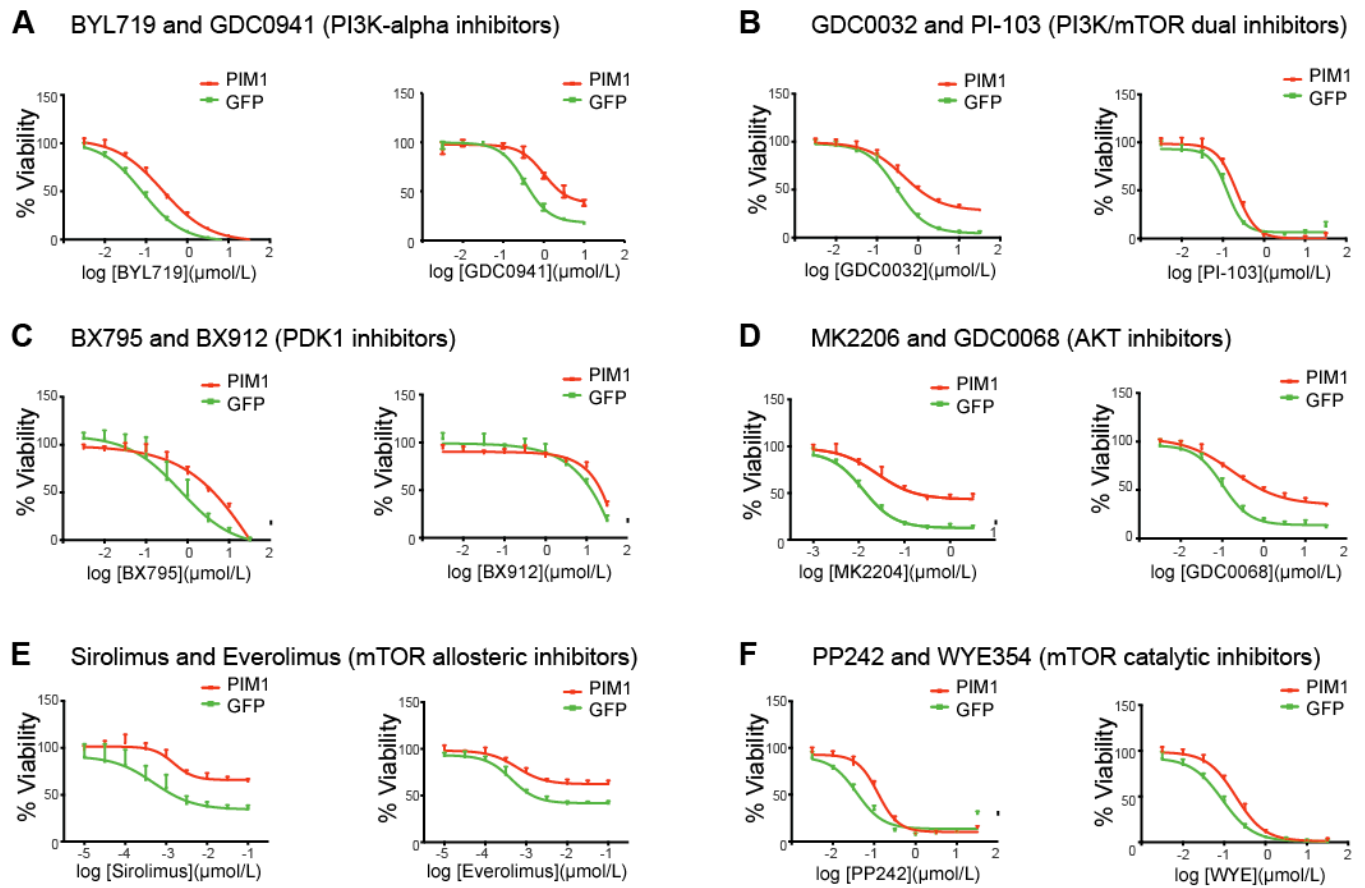
D HER2-enriched without *PIK3CA* mutation



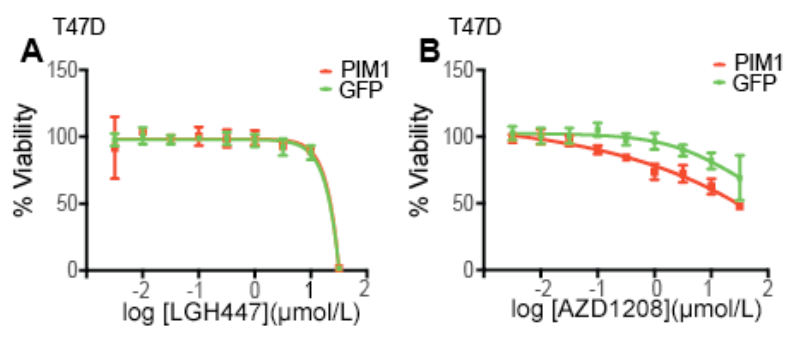
E *PTEN*-loss



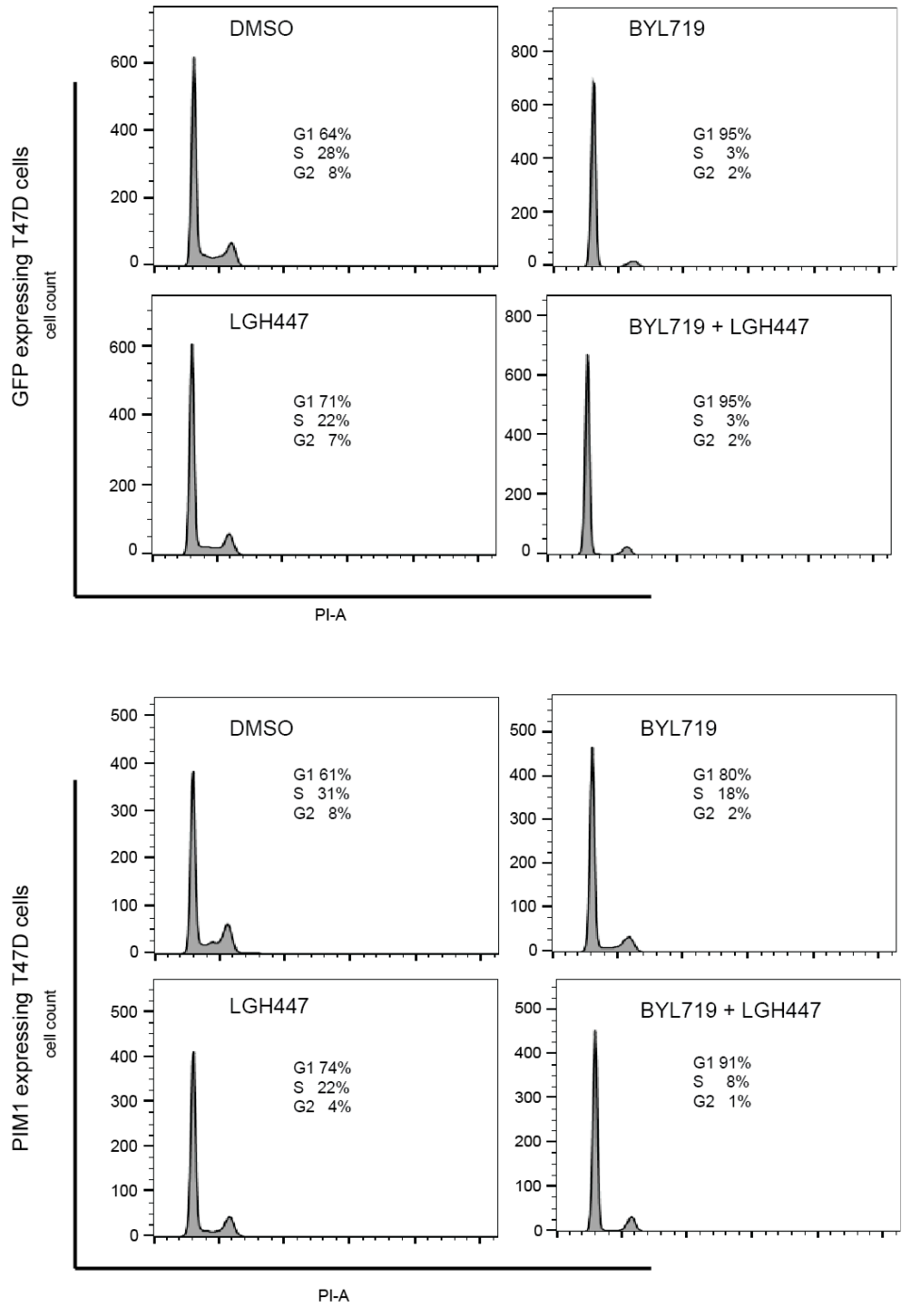
S. Fig. 3. PIM1 confers resistance to inhibitors targeting key components of PI3K pathway. T47D cells expressing GFP or PIM1 were treated with various doses of (A) BYL719 and GDC0941, (B) GDC0032 and PI-103, (C) BX795 and BX912, (D) MK2204 and GDC0068, (E) Sirolimus and Everolimus, (F) PP242 and WYE354, each for 3 days. Cell proliferation was determined by MTS assay. Mean and SE of three replicates are shown.



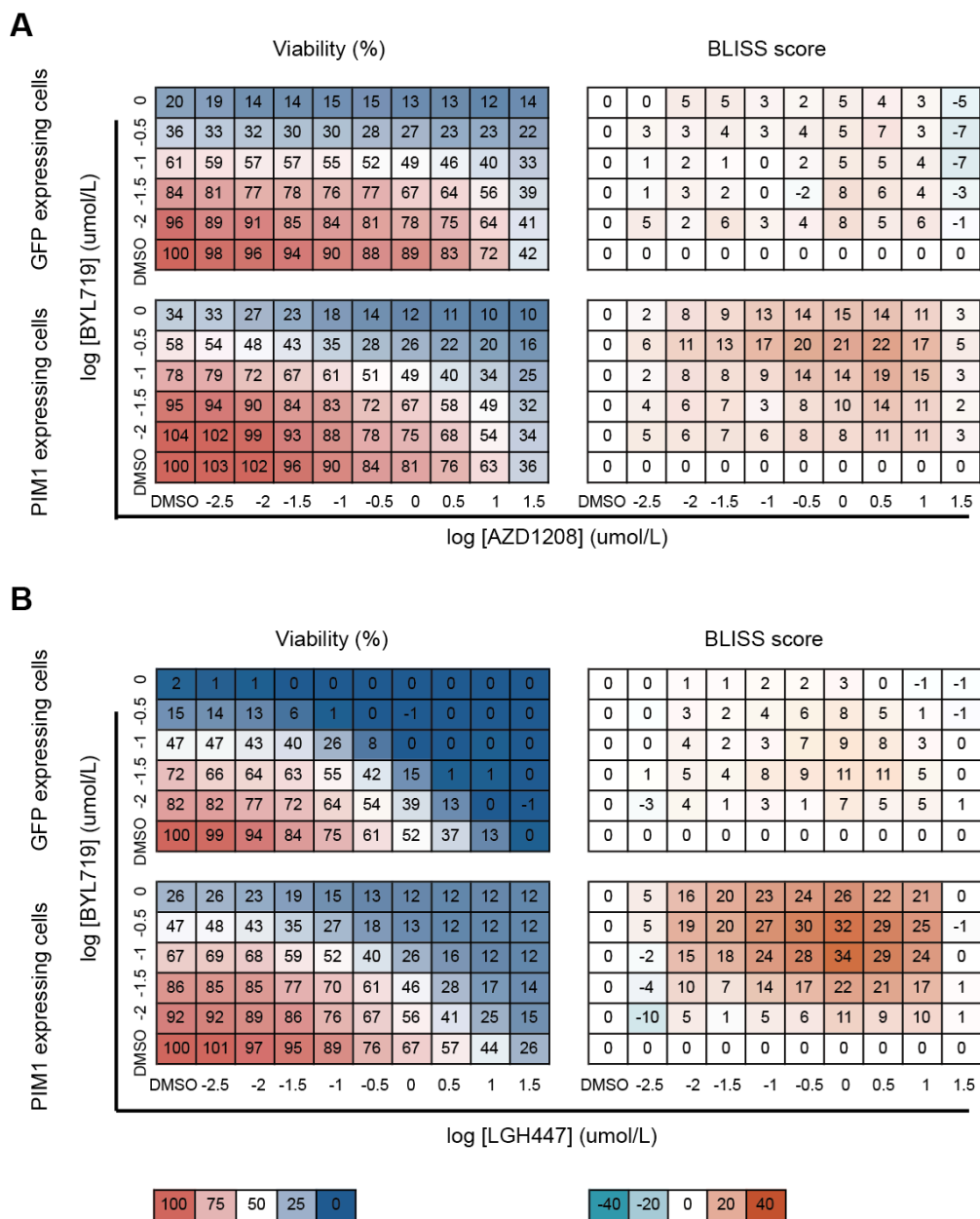
S Figure 4. PIM1 inhibitors alone have minimal inhibitory effects on T47D cells with or without PIM1 overexpression. T47D cells expressing GFP or PIM1 were treated with various doses of LGH447 (**A**) or AZD1208 (**B**) for 3 days. Cell proliferation was determined by MTS assay. Mean and SE of three replicates are shown.



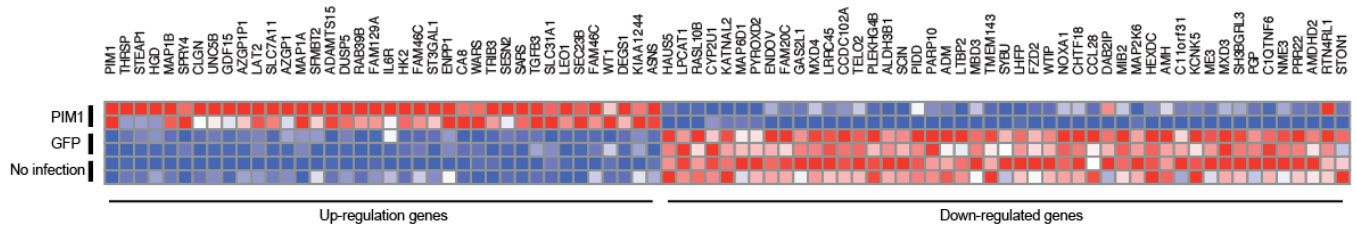
S. Figure 5. PIM1 expression abrogates cell-cycle arrest in cells treated with BYL719. T47D cells expressing GFP (top panel) or PIM1 (bottom panel) were treated with vehicle control or indicated inhibitors (BYL719 at 1uM and/or LGH447 at 1uM), fixed and staining with propidium iodide (PI). The cells were subjected to cell-cycle analysis. The representative histograms of each condition were shown. The experiment was performed in biological triplicates.



S. Figure 6. BYL719 and AZD1208 or LGH447 demonstrated synergy in PIM1 expressing T47D cells. A. GFP or PIM1 expressing T47D cells were treated with an increasing concentration of BYL719 and AZD1208 in indicated combination for 3 days. Cell proliferation was determined by MTS assay. The cell viability was shown in the left panel for each combination of doses. BLISS excess score was then calculated for each well and shown in right panel. A BLISS score > 10 indicates synergistic effect. Each combination of doses was tested in triplicates. Mean of the triplicates was used for calculation of viability and BLISS score. **B.** Same with A, except that LGH447 was used in combination with BYL719.

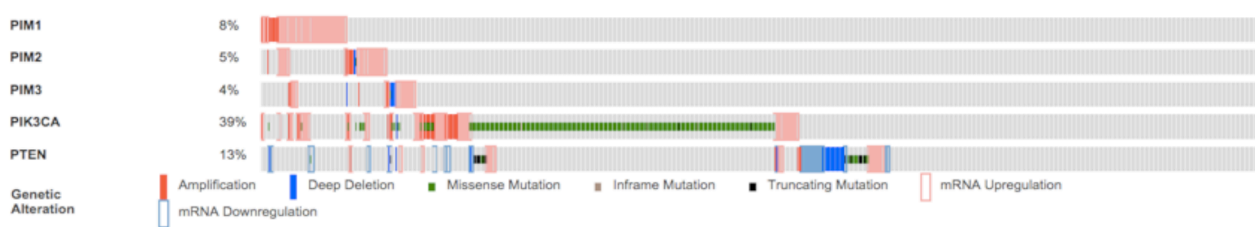


S. Figure 7. PIM activation signature. Gene expression in T47D cells with PIM1 overexpression was compared to GFP expressing cells and no infection parental cells (each in duplicate). The top 37 differentially upregulated genes together with PIM1, 2, 3, and the top 47 differentially downregulated genes (FDR<10%) were defined as PIM signature.



S. Figure 8. PIM and PI3K pathway genetic mutations showed mutual exclusivity in treatment-naïve breast cancers. A. Matrix heatmap generated using cBioPortal showing alterations of PIM family genes, PIK3CA and PTEN in the breast invasive carcinoma (TCGA, provisional) dataset. All 960 tumor samples were shown. **B.** Number of cases stratified based on the designated gene alterations. PIK3CA and PIM1 genes were queried. $p < 0.001$, Fisher exact test for co-occurrence/mutual exclusivity test. Log odd ratio = - 0.904, indicating strong tendency to be mutually exclusive. **C.** Same with **B**, except PIM1,2,3 alterations were grouped and PIK3CA/PTEN alterations were grouped. $p = 0.0015$, Fisher exact test for co-occurrence/mutual exclusivity test. Log odd ratio = - 0.616, indicating strong tendency to be mutually exclusive.

A



B

		<i>PIK3CA</i>	
		Altered	WT
<i>PIM1</i>	Altered	16	58
	WT	359	527

C

		<i>PIK3CA/PTEN</i>	
		Altered	WT
<i>PIM1,2,3</i>	Altered	48	87
	WT	417	408